SUPPORTING ONLINE MATERIAL

Instrument Detail

The Cassini Titan Radar Mapper (*S1*) is a K_u-band (13.78 GHz, λ = 2.17 cm) linear polarized radar instrument operating over a wide range of geometries and conditions in four modes. Synthetic Aperture Radar (SAR) mode operates at altitudes less than 4000 km with resolution varying from 400 m to 1 km. Images are acquired either left or right of nadir with two to seven looks. A swath of 120- to 450-km width is created from five antenna beams. In altimetry mode, the central 0.35° beam is used for time-of-flight measurements that are converted into Titan radii with relative accuracy near 35 m (actual accuracy may be larger for several reasons) and spatial resolution 20–25 km, with approximately one posting per kilometer. Scatterometry mode measures surface backscatter coefficient σ_0 variation with incidence angle at distances up to 25,000 km. Radiometry mode passively measures brightness temperature. Coverage using SAR and altimetry modes is limited by both orbital geometry and range, but scatterometry and radiometry coverage at 300–600-km resolution is increased at larger ranges by turning the entire spacecraft in a raster pattern to generate images. Nonrastered radiometry data are collected during all other modes at higher resolutions (10–20 km for SAR, 75–125 km for scatterometry). Absolute accuracy of all radiometry measurements is based on a preliminary calibration for which the uncertainty is estimated to be approximately ±5 K. Relative precision in each radiometry image is 0.1–0.2 K. SAR, altimetry, and scatterometry calibrations are still under evaluation.

Observational Geometries and Details

Fig. S1. Radar coverage diagram during Cassini's Titan T_a flyby on October 26, 2004, overlaid on top of a Cassini Imaging Science Subsystem (ISS) map of Titan's surface. The orange circles are inbound scatterometry coverage. The white strip is SAR ground tracking running from left to right in time, with a turn to altimetry at the end. The yellow line is the ground tracking of outbound altimetry. The magenta and green circles are the coverage of the outbound scatterometry and radiometry, respectively. The time interval between the data points is 1 second for SAR and altimetry, and 5 seconds for scatterometry and radiometry.

Table S1. Key Transition Times for T_a

	Epoch Relative Time	UTC Time (2004-10-26)
Inbound Scatterometry (Scatt)		
Scatt mode begins	-1:20:00	14:10:09
Nadir pointing begins	-1:19:30	14:10:49
Nadir pointing ends	-1:18:50	14:11:19
Scatt scan begins	-1:16:39	14:13:30
Off-target sweep for calibration	-0:46:34	14:43:35
Scatt mode ends	-0:44:00	14:46:09
Synthetic Aperture Radar (SAR)		
SAR Hi mode begins	-0:04:30	15:25:39
Closest approach—turn to DLAP* begins	0:00:00	15:30:09
DLAP profile tracking begins	0:01:00	15:31:09
SAR Low mode begins	0:05:15	15:35:24
DLAP profile tracking ends, slew to nadir begins	0:14:00	15:44:09
SAR Low-mode 8-bit straight begins	0:14:00	15:44:09
SAR Hi-mode beam-3 only begins	0:16:00	15:46:09
Outbound Altimetry (Alt)		
Alt mode begins	0:19:00	15:49:09
Nadir pointing begins	0:19:40	15:49:49
Alt mode ends	0:30:00	16:00:09
Outbound Scatterometry		
Attenuator engineering tests begin	0:30:00	16:00:09
Slew to scatt scan begins	0:30:20	16:00:29
Scatt mode begins	0:30:36	16:00:45

Off-target sweep for calibration	1:12:30	16:42:39
Nadir-pointed stare begins	1:15:00	16:45:09
Compressed scatt mode begins	1:16:00	16:46:09
Scatt mode ends	1:22:00	16:52:09
Outbound Radiometry (Rad)		
Rad mode begins	1:22:00	16:52:09
Slew to rad scan (1st polarization) begins	1:40:00	17:10:09
Slew to rad scan (2nd polarization) begins	3:27:00	18:57:09
Rad mode ends	4:52:00	20:22:09
*DLAP: Desired-Look-Angle Profile spacecraft maneuver required for SAR imaging.		

Fig. S2. SAR image sampled at 128 pixels/degree (351 m/pixel), preserving essentially the full resolution of the data. Normalization, scaling, and map projection (apart from scale) are identical to Figure 1 in the printed article.

Fig. S3. Global map of backscatter cross-section from both inbound and outbound scatterometry observations, normalized to a model backscatter curve as described in printed text, logarithmically scaled, and overlaid in color on an ISS map of Titan.

Fig. S4. Global map of brightness temperature variations, divided by a Fresnel emissivity to reduce variations due to emission and polarization angles, and overlaid in color on an ISS map of Titan. Only observations obtained at emission angles ≤55° (during scatterometry) and ≤50° (radiometry only) are included. Calibration of absolute instrument sensitivity and relative gains for different operational modes and sequences is preliminary. Results have therefore been expressed as deviations from a representative temperature. Note inverted color scale relative to Figure S2.

Resurfacing Rate

Volcanism, the expulsion of fluid material from the interior of a body, is driven by internal heat. We do not yet know enough to consider specific eruption mechanisms, but energy arguments and the lack of craters lead us to posit a cryovolcanically active Titan. Geothermal heat flow from radioactive decay of its rocky interior, augmented by internal tidal dissipation and a comparable residual amount from secular cooling, would be ~6 mWm^{-2} (*S2*, *S3*), about 10% of that for present-day Earth. Because the rocky material within Titan is likely confined to a deep-seated core, the estimated heat flow leads to the expectation that Titan's volcanism involves water. In this model, water ice is the bulk of Titan's mantle, perhaps with additional contaminants like ammonia that lower the freezing point, density, and mobility of the melt (*S4*, *S5*). On Earth, about 10% of the total heat flow is expressed as the latent and sensible heat of molten silicate lava (~1.9×10^6 Jkg^{-1}), yielding a resurfacing rate of 0.05 mm/yr or equivalently about 20 km^3 of lava per year in total. Applying the same calculation (10% of heat flow expressed as volcanism, [*S6*, *S7*]) to Titan yields essentially the same resurfacing rate as that of Earth, taking a latent heat for ice of ~10^5 Jkg^{-1} and a specific heat of ~2000 $Jkg^{-1}K^{-1}$ with ΔT ~100 K and thus a magma heat content of 3×10^5 Jkg^{-1}. Over Titan's smaller area, this corresponds to 50 m of "cryolava" deposited per 10^6 yr globally. This resurfacing rate is two orders of magnitude higher than the estimated deposition rate of photochemical materials on Titan (~1 km over 4.5 Gyr ~0.2 m/10^6 yr [*S8*]). The youthful appearance of Titan in the first radar coverage is consistent with this model. Though relatively high, the resurfacing rate just calculated casts doubt on the conclusion that the flow feature in Fig. 2E of the printed text is ~1 km thick, as suggested by radarclinometry. The flow is approximately 200 × 70 km, and would have a volume on the order of 10^4 km^3 if it were this thick. Such a volume represents >2000 years of Titan's global cryolava production.

Radarclinometry Methods

Radarclinometry is the equivalent, using radar imagery, of photoclinometry, or shape-from-shading (*S9*). Results reported here have been derived by a simple, one-dimensional profiling technique in which backscatter values on a profile across a feature are interpreted as resulting from slopes toward or away from the spacecraft, and these slopes are integrated to yield an elevation profile. The implementation used is based on that for photoclinometry reported in (*S10*). The features of interest are geometrically simple, so radarclinometry approaches that yield a topographic model over a two-dimensional region (*S9*) are not essential. Given the strong non-slope-related variations in backscatter seen in on Titan, it is also easier to find one-dimensional traverses than two-dimensional regions with uniform backscatter as required to apply the method. The estimation of slopes from backscatter includes both the surface-scattering law and the variation in the area of a pixel depending on its orientation. A scattering law of the form $\sigma_0 \propto 1/\sin(i)$ is used, with the constant of proportionality (i.e., σ_0 at a specific incidence angle i) chosen independently for each feature modeled in order to yield a profile that returns to its original level after crossing a discrete feature such as a hill or flow. The amplitude of the estimated relief depends on the assumed scattering law, but only rather weakly. Because of the pixel-area factor, the slopes and heights reported would increase only by roughly a factor of two even if the scattering law were completely flat at the incidence angles of interest. A more plausible estimate of the uncertainty in the feature heights is a few tens of percent.

SOM References

S1. C. Elachi *et al*., *Proc. IEEE* **79,** 867 (1991).

S2. R. Lorenz, *Planetary and Space Science* **45**, 1009 (1997).

S3. O. Grasset, C. Sotin, F. Deschamps, *Planet. Space Sci.* **48**, 617 (2000).

S4. F. Sohl, H. Hussmann, B Schwentkter, T. Spohn, R. Lorenz, *J. Geophys. Res.* **108**, 5130 (2003).

S5. J. Kargel, S. Croft, J. Lunine, J. Lewis, *Icarus* **89**, 93 (1991).

S6. S. Croft, J. Lunine, S. Kargel, *Icarus* **73,** 279 **(**1988).

S7. P. Francis, *Volcanoes: A Planetary Perspective* (Oxford Univ. Press, New York, 1993), p.3.

S8. R. Lorenz, *Planetary and Space Science* **44**, 1021 (1996).

S9. R. Kirk, Ph.D. Thesis [unpubl.], Calif. Inst. Tech., pp. 165–258 (1987); R. Kirk, J. Barrett, L. Soderblom, paper presented at ISPRS Workshop "Advances in Planetary Mapping 2003," Clear Lake, TX, 22 March 2003, abstract online at http://astrogeology.usgs.gov/Projects/ISPRS/Meetings/Houston2003/abstracts/Kirk_isprs_mar03.pdf

S10. L. Soderblom, R. Kirk, K. Herkenhoff, paper presented at the 33rd Annual Lunar and Planetary Science Conference, League City, TX, 11–15 March 2002, abstract no. 1254.

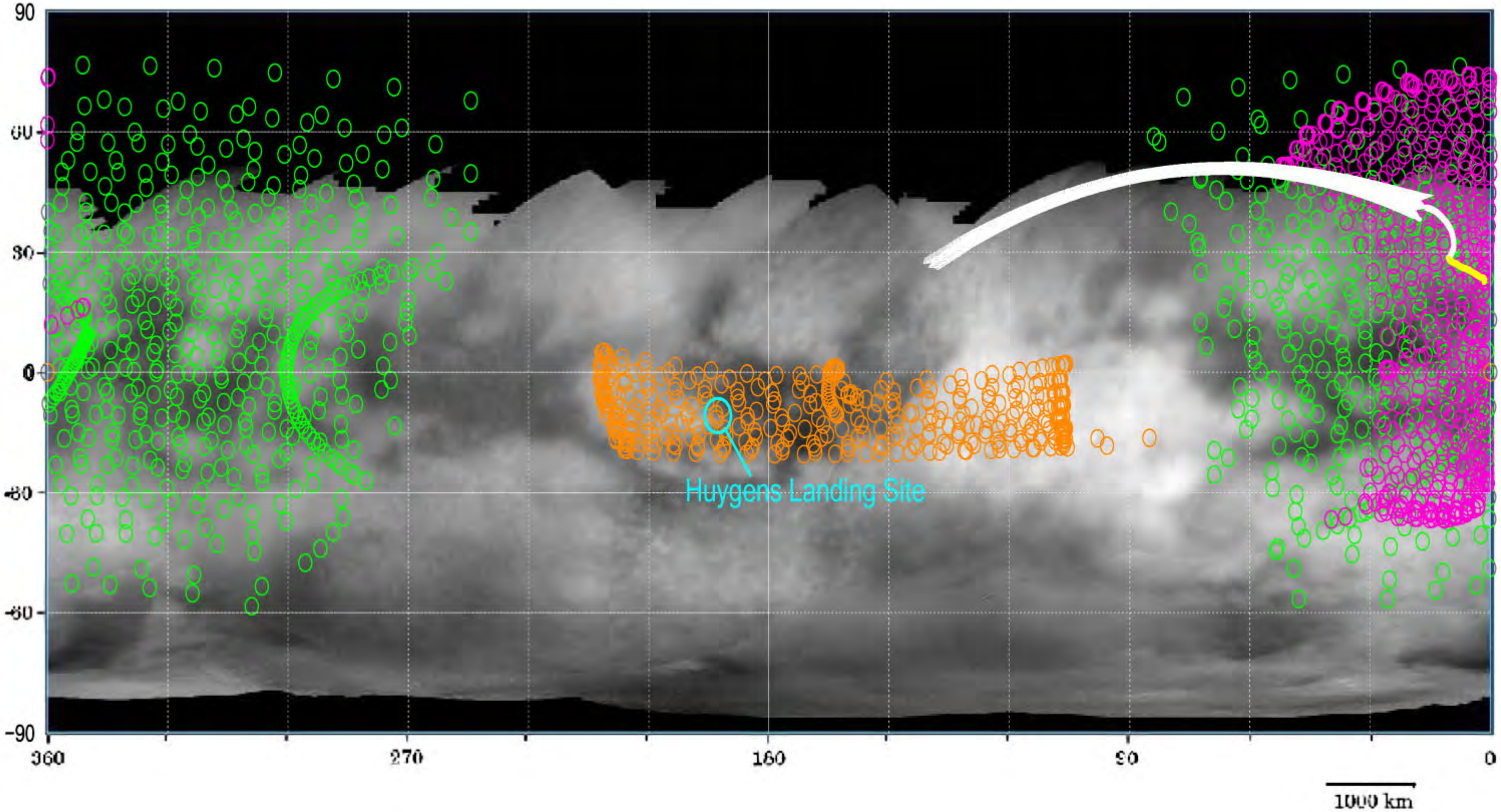

90
60
30
0
-30
-60
-90
360
270
180
90
0
Huygens Landing Site
1000 km

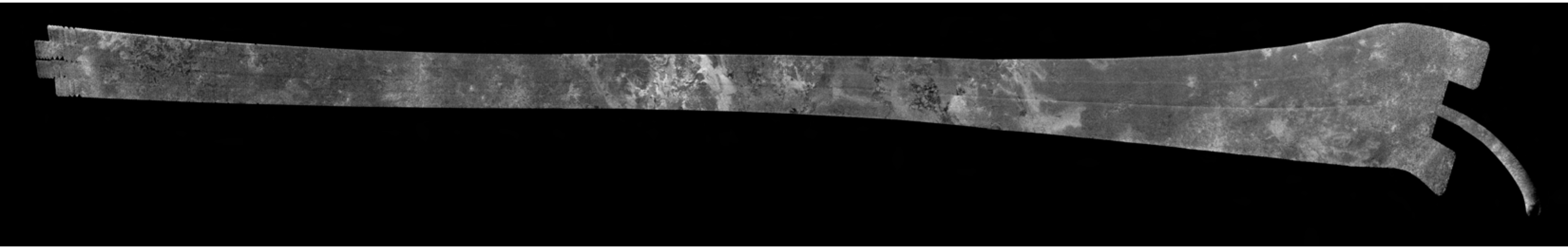

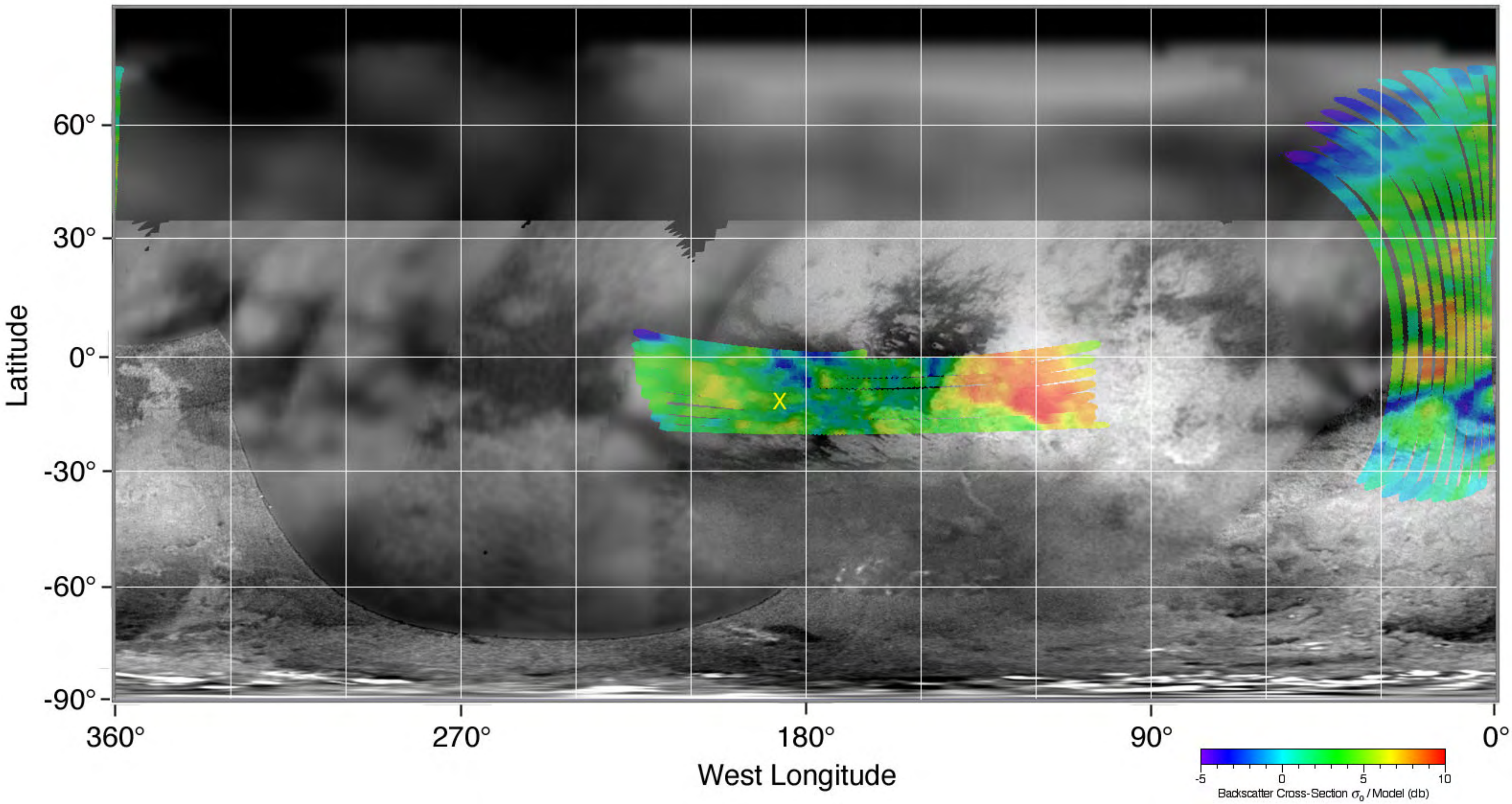
60°
30°
0°
-30°
-60°
-90°
Latitude
360°
270°
180°
90°
0°
West Longitude
X
-5
0
5
10
Backscatter Cross-Section σ_0 / Model (db)

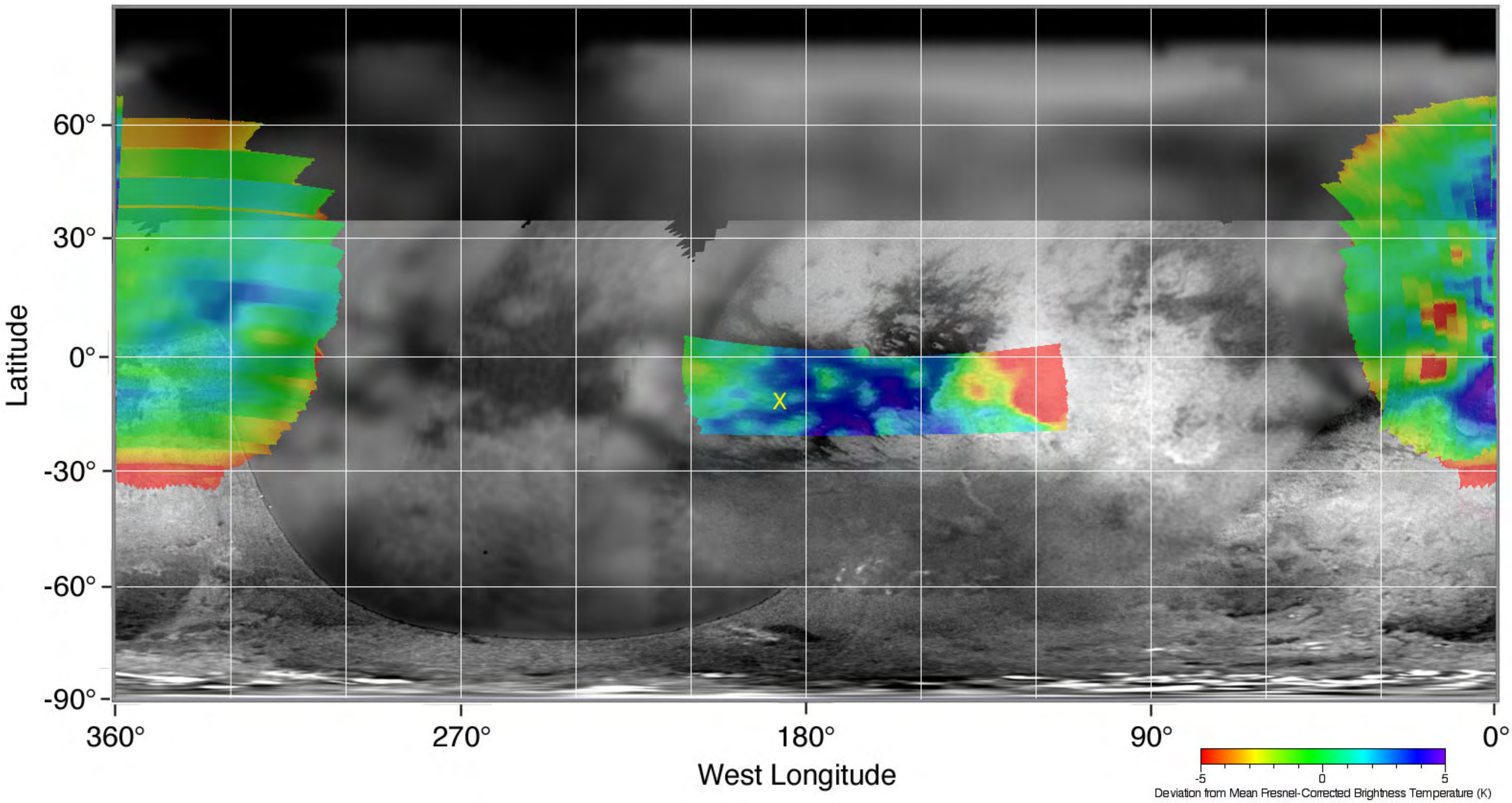

60°
30°
0°
-30°
-60°
-90°
Latitude
360°
270°
180°
90°
0°
West Longitude
X
-5
0
5
Deviation from Mean Fresnel-Corrected Brightness Temperature (K)